

# Experimental Demonstration of a Statistical OFDM-PON with Multiband ONUs and Elastic Bandwidth Allocation

Iván N. Cano, Xavier Escayola, Philipp C. Schindler, María C. Santos, Victor Polo, Juerg Leuthold, Ioannis Tomkos, and Josep Prat

**Abstract**— The statistical OFDM-PON concept with multiband Optical Network Units (ONUs) is experimentally tested with two users and an Optical Line Terminal (OLT) at 2.5 / 5 Gb/s total effective capacity with BPSK/QPSK modulation. Both downstream (DS) and uplink (UL) were measured based on intensity modulation and direct-detection (IMDD). The ONUs consisted of local non-preselected wavelength distributed feedback (DFB) laser sources centrally controlled to reduce overlapping probability. In addition, a radiofrequency (RF) mixing stage in the ONUs up/down-converts the user data to/from the OFDM signal reducing the computational effort. Compared with ONUs processing the whole signal, the multiband approach presents comparable results with almost symmetrical power budgets of around 25dB and 20dB with BPSK and QPSK respectively, which could increase up to 4.5dB by allocating a spectral guard interval between the optical carrier and the OFDM data. Furthermore, elastic bandwidth allocation is explored which is shown to compensate for up to 18dB differential link-loss.

**Index Terms**—Passive optical networks; PON; Orthogonal Frequency Division Multiplexing; OFDMA-PON; statistical-PON; elastic bandwidth allocation; Intensity modulation direct-detection

## I. INTRODUCTION

Orthogonal frequency division multiplexing access

Manuscript received July 1, 2014.

Iván N. Cano, Xavier Escayola, María C. Santos, Victor Polo and Josep Prat are with Universitat Politecnica de Catalunya (UPC), Jordi Girona 1-3, E-08034, Barcelona, Spain (e-mail: ivan.cano@tsc.upc.edu).

Philipp C. Schindler was with Institute of Photonics and Quantum Electronics, Karlsruhe Institute of Technology, 76131, Karlsruhe, Germany and now is with Infinera Corp, Sunnyvale, CA, USA.

Juerg Leuthold was with Institute of Photonics and Quantum Electronics, Karlsruhe Institute of Technology, 76131, Karlsruhe, Germany and now is with Laboratory for Electromagnetic Fields and Microwave Electronics (IFH), Swiss Federal Institute of Technology Zurich (ETHZ).

Ioannis Tomkos is with Athens Information Technology Center (AIT), 19.5km Markopoulo Ave., Peania 19002, Athens, Greece.

(OFDMA) has attracted interest for research in passive optical networks (PON) due to features like fine bandwidth (BW) granularity and elastic BW provisioning [1-4]. Several studies have shown its feasibility for downstream (DS) though few have been related to the uplink (UL) multipoint-to-point. In [5, 6], an UL with centrally distributed optical carrier and coherent detection was demonstrated. As an alternative to reduce the cost of the optical network units (ONU) a statistical network with direct-modulated non-preselected light sources was proposed [7-9]. In [7], the concept was studied in an OFDM-PON through statistical analysis and numerical simulation. It included a centralized thermal tuning control of random wavelength ONU lasers to reduce overlapping probability and limit interference.

In current PON deployments, each ONU processes the complete signal BW even if the user employs only a fraction of it. This overcapacity in the ONU has an effect on the power consumption [10]. In order to reduce the ONU complexity and lower its energy requirements, a multiband OFDM approach can be employed. In this technique, the ONUs include tunable radio-frequency (RF) oscillators to place/retrieve the assigned subcarriers (SC) to/from the multiuser OFDM signal [11, 12].

A system requirement demanded by operators for future PON is to reuse legacy network infrastructure. Hence, the differential link-loss among the users spread geographically from the central office becomes a major challenge [13]. In OFDM-PON, this concern can be addressed through dynamic assignment of SC and modulation levels to the users according to their power budget availability [14].

This paper experimentally validates a statistical multiband OFDM PON with two ONUs in both DS and UL including flexible BW allocation. It extends the results presented in [12] where only the UL was studied. It also compares the performance between the system in baseband and with a spectral guard interval (GI) between the optical carrier and the OFDM data signal. The technique reduces the processing effort in the ONU by setting their allocated BW into non-overlapping orthogonal frequency bands by means of a RF mixing stage. As a result, the fast Fourier transform (FFT) size in the ONU is decreased. Proper detection of data to/from both ONUs is achieved in DS/UL with performance values in line with those measured with digital SC allocation. In addition, the flexible BW allocation is also studied to compensate the difference in losses

experienced by the users in the PON. The paper is organized as follows: a description of the network architecture with the statistical PON concept is presented first; the experimental setup is then described followed by the results and the conclusions.

## II. NETWORK ARCHITECTURE: THE STATISTICAL OFDM-PON CONCEPT

A power splitter based PON tree architecture with service spectrum breakdown such as the Accordance network proposal [6] is considered (Fig. 1). Both the optical line terminal (OLT) and ONUs are based on intensity-modulation with direct-detection (IMDD) technique whose simplicity and performance is attractive for access networks [15-17]. In order to avoid backscattering effects, DS and UL are assigned to L-band and C-band respectively.

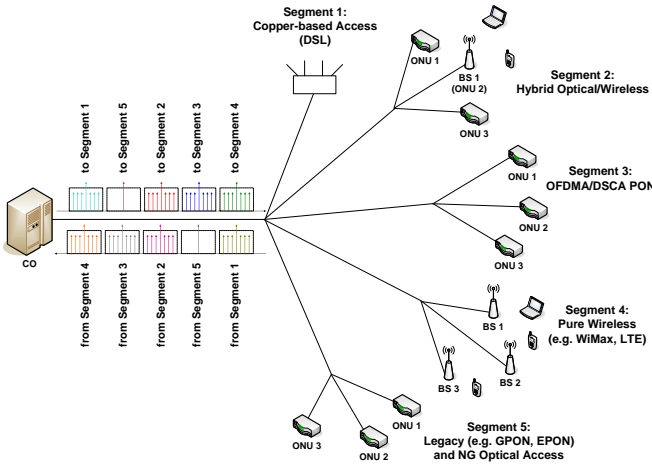


Fig. 1. Network architecture.

The ONU transmitter (Tx) consists of distributed feedback lasers (DFB) with non-preselected wavelength in the C-band. The use of such light sources would evade large inventory and complex provisioning to the operator. To avoid interference, the emission frequency of the ONU laser

is regulated through temperature and current control circuits which allows for  $\lambda$  shifts up to 1.6nm with 0.1nm steps. The tuning transition time is reduced to 2 $\mu$ s approximately by employing current transients and temperature changes simultaneously [18].

The OLT includes an intelligent activation and operation algorithm like those proposed in [19, 20] to initialize and track the  $\lambda$  of the ONUs lasers by centrally measuring and sending instructions to the control circuits. As a result, the ONU rejection probability is minimized [7]. The ONUs  $\lambda$  are kept at enough spectral distance (0.1nm) to reduce the optical beat interference (OBI) at the OLT below a quality threshold. Since the ONU lasers emit at random wavelengths and are centrally managed to maintain the overall performance, it is referred as statistical PON.

## III. EXPERIMENTAL SETUP

The setup contained an OLT and two ONUs emulating a PON as depicted in Fig. 2. For the OLT Tx a total of  $2^{19}$  bits were randomly generated and mapped to either binary phase-shift keying (BPSK) or quadrature-PSK (QPSK). The symbols were arranged to have Hermitian symmetry in a 256-point inverse Fast Fourier Transform (iFFT) to get a real valued OFDM signal. This FFT size was chosen because it is currently achievable in FPGA real-time processing [21]. No cyclic prefix was added since for the fiber lengths considered no significant chromatic dispersion was generated. The first half of the BW carried the DS information of ONU<sub>1</sub>, whereas the second were filled with ONU<sub>2</sub> DS data. The OFDM signal was loaded to an arbitrary waveform generator (AWG) which produced samples at 5GSa/s with 8-bits resolution digital-to-analog converters (DAC). This entailed a maximum effective capacity of 1.25Gb/s for each user with BPSK modulation and of 2.5Gb/s with QPSK. The electrical output was amplified and modulated a DFB emitting at 1600.85 nm through a Mach-Zehnder modulator (MZM) biased at quadrature with an insertion loss of almost 6dB. The optical output power was limited to 0dBm. The optical signal was then sent to the optical distribution network (ODN) after a

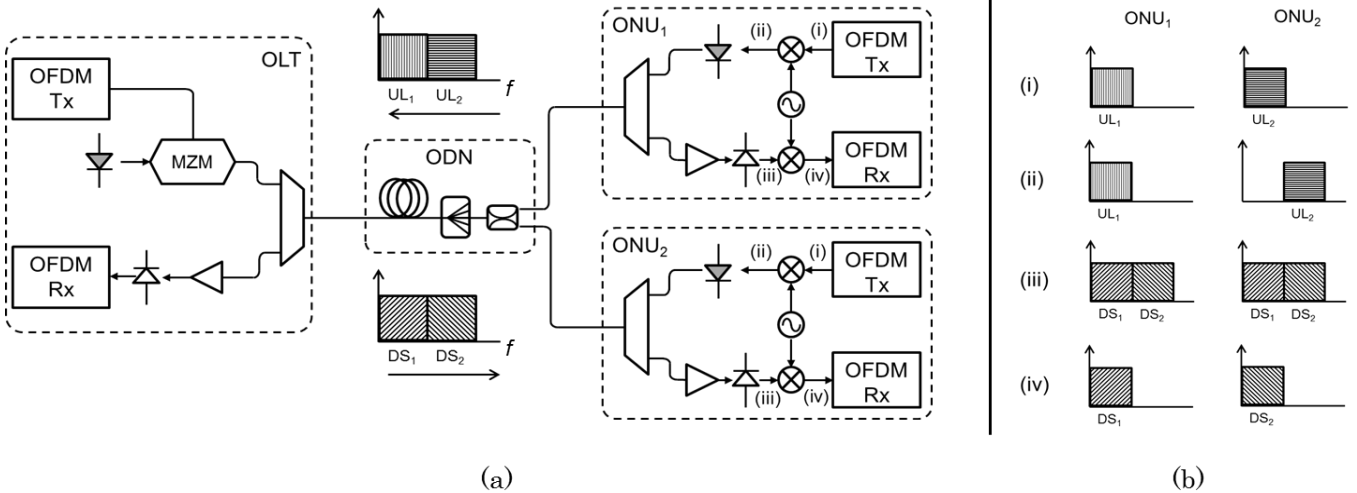


Fig. 2. (a) Experimental setup block diagram; (b) Representation of the data spectra in ONU<sub>1</sub> and ONU<sub>2</sub>.

red/blue filter.

The OLT Rx involved a single 10GHz photodiode (PD) preceded by an erbium doped fiber optical amplifier (EDFA) which kept the input optical power to the PD at -9dBm. The signal was then sampled with a 50GSa real time oscilloscope (RTO). The digital samples were demodulated with a 256-point FFT, followed by a 1-tap equalizer whose coefficients were set by a known training sequence in the initial four OFDM symbols and the bit error ratio (BER) for each ONU UL signal was computed.

The ODN entailed 25km of single mode fiber, an optical attenuator of 12dB and a 3dB optical coupler. The total loss of the ODN was 20dB. In Fig. 2 a representation of the transmitted spectra in the PON is shown.

At the ONUs, the Tx generated  $2^{18}$  random bits which were mapped to either BPSK or QPSK, accommodated for Hermitian symmetry and modulated with a 128-point iFFT each. The UL samples of each ONU were loaded separately to two channels of an AWG with 8-bit resolution. Each user signal had 2.5GHz BW. The resulting baseband signals were shifted to their corresponding frequency slot through an RF mixer (Fig. 2b) and then directly modulated a DFB laser with 5GHz BW. The output power of each ONU was set to 0dBm. The optical Tx signal passed through a red/blue filter and it was joined in a 3dB optical coupler with the contribution from the other ONU. The total UL capacity was thus equal to that of the DS signal. Then, the composite OFDM UL signal was launched into the ODN towards the OLT where it was detected. As for the ONU Rx, after the red/blue filter, the isolated DS component was detected by a p-i-n PD preamplified by a semiconductor optical amplifier (SOA) with 18dB gain and noise figure (NF) of 6.5dB. Alternatively, for simplifying the Rx, we also tested an avalanche PD (APD). An RF down-conversion stage then took the DS spectrum corresponding to the ONU down to baseband. The electrical signal was low-pass filtered and sampled with a 50GSa RTO. The samples were demodulated with a 128-points FFT, equalized, demapped and the BER was computed.

#### IV. RESULTS

We first emulated the activation process in the statistical PON with efficient optical BW occupation. We tuned ONU<sub>2</sub>  $\lambda$  to transmit as close as possible to ONU<sub>1</sub> while limiting the OBI below a minimum value [22-24]. The original and final wavelengths are shown in Fig. 3.

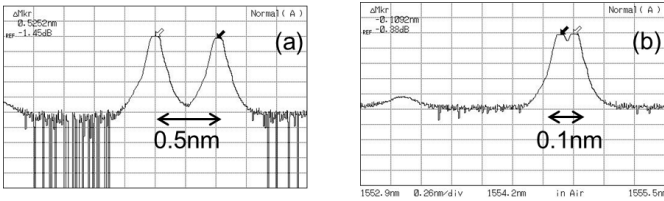


Fig. 3. (a) Initial and (b) final  $\lambda$  separation between ONUs.

Initially, ONU<sub>1</sub> and ONU<sub>2</sub> emitted at 1554.7nm and 1554.2nm respectively. ONU<sub>1</sub> was first connected to the PON and afterwards ONU<sub>2</sub> was turned on (Fig. 3a). As measured in [7, 23], a spectral separation of 0.1nm between

users was enough to avoid penalties. To use optical BW more efficiently, ONU<sub>2</sub> was tuned to displace its emission  $\lambda$  rapidly by 0.4nm to 1554.6nm (Fig. 3b) where the reception quality was maintained [7, 23].

#### A. Downstream

The DS signal was generated with a single FFT at the OLT. The lower and higher half of the spectrum were reserved for ONU<sub>1</sub> and ONU<sub>2</sub> respectively. Each ONU then detected the complete optical signal but processed only its corresponding SC.

As a first test, both ONUs equally shared the available SC. The frequency of the RF mixer in ONU<sub>2</sub> ( $f_{IF2}$ ) was set to 1.25GHz. ONU<sub>1</sub> did not need any RF stage as it was assigned the lowest spectral band in the OFDM signal, which started at baseband. Then each ONU only processed their own half of the SC. Fig. 4 plots the BER against the Rx power for both ONUs with BPSK and QPSK modulation. At a forward error correction (FEC) target of BER= $10^{-3}$ , both ONUs detected at approximately -25dBm and -20dBm the BPSK and QPSK signal respectively. Considering that  $P_{Tx}=0$ dBm, the power budget available was 20dB and 25dB for QPSK and BPSK correspondingly. The difference in the Rx power between the modulation formats could give the possibility to switch them according to the power budget available and BW demand of each user. The small difference observed in the Rx sensitivities among the ONUs was mainly caused by small drifts in ONU<sub>2</sub> RF oscillator.

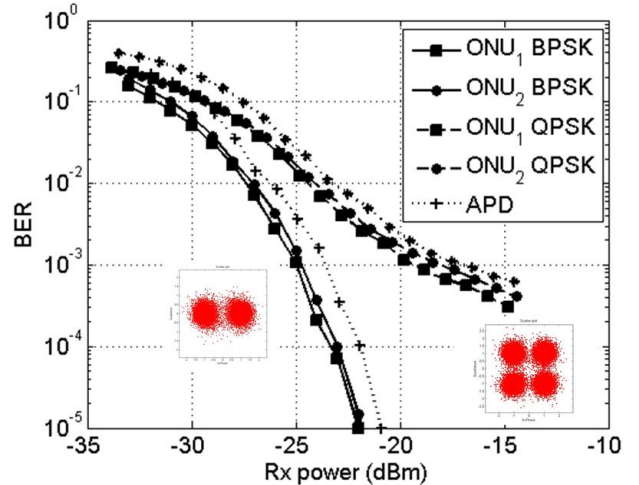


Fig. 4. BER against Rx power for the two ONUs equally sharing the total BW with BPSK and QPSK modulation in DS. The dotted lines correspond to the averaged curves of both ONUs with APD-based Rx. The constellations are for BER= $10^{-3}$  in ONU<sub>1</sub>.

Since the ONU is a cost-sensitive element in the PON, we replace the preamplified PD in Rx with an APD (FRM5N143DS). Fig. 4 includes the averaged performance graphs over both ONUs when employing the APD with BPSK and QPSK. There is a penalty of about 1.5dB for the APD Rx for both modulation formats. However, the power budget can be kept by increasing the launched power to 2dBm with the advantage of a simpler ONU Rx.

In a second set of experiments, a spectral bandgap (BG) with empty SC was considered between the data spectrum of ONU<sub>1</sub> and ONU<sub>2</sub>. We left unchanged  $f_{IF2}$  and discarded

the unused SC in each ONU after demodulation. The effective BW per ONU ( $BW_{ONU}$ ), measured as the operative SC by the total available, was thus, reduced. The Rx sensitivity at  $BER=10^{-3}$  against  $BW_{ONU}$  for both ONUs is shown in Fig. 5 with BPSK and QPSK modulation.

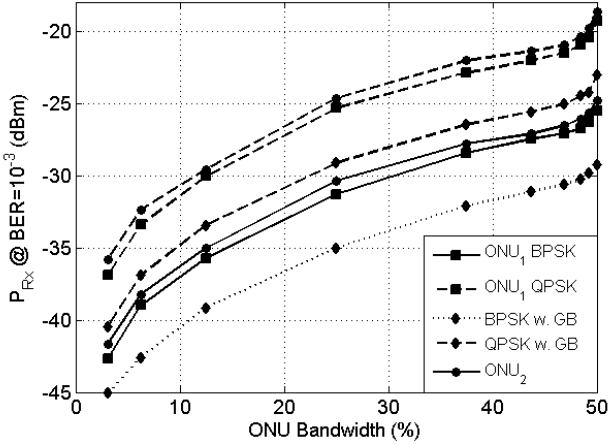


Fig. 5. Rx sensitivity at  $BER=10^{-3}$  against effective data BW for both ONUs with BPSK and QPSK modulation formats with multiband OFDM. The dotted lines correspond to  $ONU_1$  curves with a spectral GI.

We observed that as the  $BW_{ONU}$  decreased, the Rx sensitivity improved. A value of  $P_{Rx}=-32$  dBm was reached when each ONU employed only 25% of the BW with BPSK. Furthermore, QPSK could be detected with only around 4.5 dB penalty as compared with BPSK. We also noticed from Fig. 5 that  $ONU_2$  had almost 1 dB penalty with respect to  $ONU_1$  which was attributed to small drifts in the electrical oscillator frequency whose tolerance was limited to  $\pm 5$  kHz [14].

When the OFDM signal is direct-detected, there are mixing terms between the SC that appear in the data frequency band degrading the performance. A spectral GI between the optical carrier and OFDM signal equal to the signal BW is typically used to keep the mixing terms out of the data band [25]. In our setup, the maximum oscillator frequency of the RF stages is 6 GHz. This entails a maximum GI of 3.5 GHz in the DS signal. An RF stage is added in the OLT and  $ONU_1$   $f_{IF1}$  is also tuned to 6 GHz.  $ONU_2$  is not used because  $f_{IF2} > 6$  GHz is required. Fig. 5 includes the Rx sensitivity curve of  $ONU_1$  with GI. There is an improvement of nearly 4.5 dB for both BPSK and QPSK. However, this enhancement comes at the expense of a wider spectrum in the OFDM signal,

For comparison, we carried out the same experiment with ONUs processing the complete DS signal, i.e. with a 256-point FFT. For the BER computation each ONU considered only its corresponding half of SC, and the rest were discarded. The obtained results (plotted in Fig. 6) were comparable with those in Fig. 5 for multiband OFDM. The latter presented a penalty for  $BW_{ONU} > 45\%$  due to the non-ideal low-pass filter response after the RF stage in Rx.

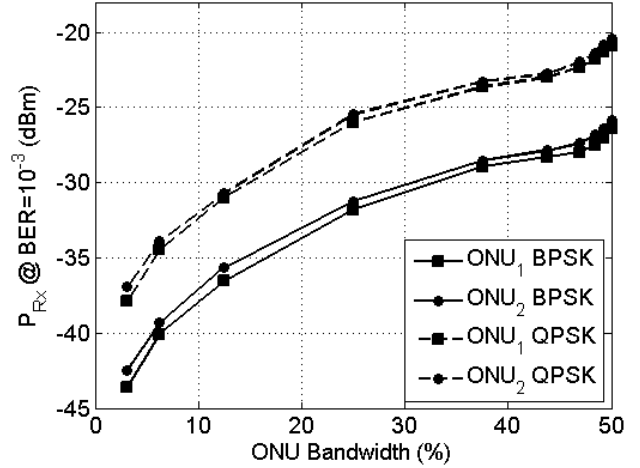


Fig. 6. Rx sensitivity at  $BER=10^{-3}$  against effective data BW for both ONUs with BPSK and QPSK modulation formats when the ONUs process the whole BW.

### B. Uplink

For the UL performance assessment, the multiband OFDM contributions of both ONUs were detected with a single 256-point FFT in the OLT. In order to reuse the electrical oscillator, the SC assignment followed the same scheme as in DS. Since the ONUs UL spectra had to be accurately synchronized, we carefully set identical electrical and optical paths between the 3 dB optical coupler and the ONUs electrical Tx generator. In a commercial network, the ONUs could be coordinated through the ranging protocol during the activation process. Fig. 7 plots the BER against the Rx sensitivity computed at the OLT for both ONUs with BPSK and QPSK modulation.

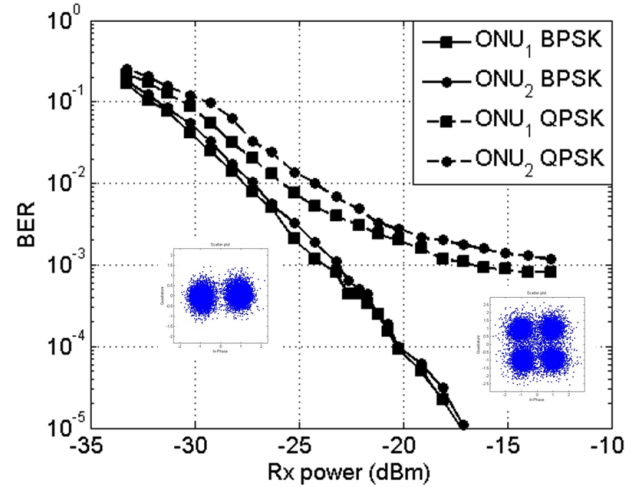


Fig. 7. BER against Rx power for both ONUs with BPSK and QPSK modulation. The constellations are for  $ONU_1$  at  $BER=10^{-3}$ .

Both ONUs were detected properly below the target  $BER=10^{-3}$  at  $-24$  dBm and  $-18$  dBm for BPSK and QPSK respectively. However, there was a BER floor appearing in the QPSK signal close to  $BER=10^{-3}$ . The same was observed for the BPSK signal but the floor was below  $BER=10^{-5}$ . This motivated to look for the errors in each SC. Fig. 8 shows the number of errors against the SC number for both ONUs. Interestingly, the errors occurred in the SC closest to the

other ONU part caused by a slight overlapping due to the spectrum tails, as seen in the inset of Fig. 8.

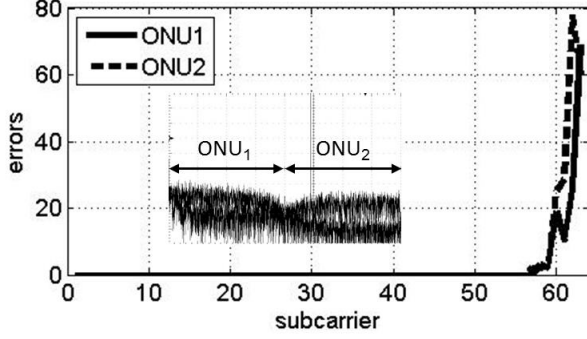


Fig. 8. Total errors against SC number.

In order to improve the performance, a spectral BG was set between the ONU signals. Each ONU occupied 25% of the BW and both were spectrally together firstly. Then ONU<sub>2</sub> spectrum was separated from ONU<sub>1</sub> by tuning  $f_{IF2}$ . The OLT processed both the ONUs data spectra and the BG. The Rx sensitivity at BER=10<sup>-3</sup> for both ONUs is plotted against the spectral BG in Fig. 9. For a 3dB penalty, a 6.25% frequency BG, i.e. 312MHz, is needed for QPSK. This value is reduced to a moderate 1.56% (78MHz) for BPSK because of its lower signal to noise ratio (SNR) requirement.

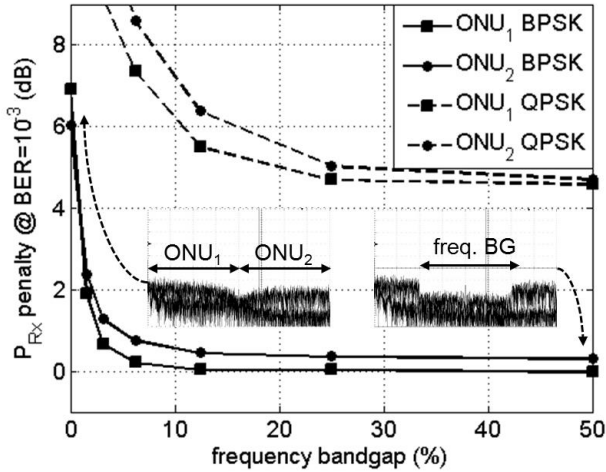


Fig. 9. Rx power for BER=10<sup>-3</sup> against frequency BG. The insets illustrate the increase of the frequency BG between the ONU contributions.

The elastic BW allocation was also evaluated in UL. The BW occupied by each of the ONUs was lowered by zero-padding (ZP) some of the SC. As a result, the spectral separation between the users was also increased improving the Rx sensitivity. Fig. 10 shows the Rx optical power needed at BER=10<sup>-3</sup> for both ONUs against BW<sub>ONU</sub> with BPSK and QPSK modulation. As expected from Fig. 9 results, there were penalties for BW<sub>ONU</sub> > 45% due to spectral overlapping in the neighboring user SC (insets of Fig. 10). Notably, the curves are similar to the ones obtained for the DS case. Due to the limited BW of the DFB lasers, a spectral GI was not tested in the UL. However, a performance improvement is expected if a spectral GI is left

between the OFDM signals and the optical carriers provided that the frequency separation between the users is correspondingly increased to prevent OBI.

When increasing the ZP, besides enlarging the spectral BG, the total power is distributed into fewer SC, increasing their SNR. Hence, clearer constellations and improved Rx sensitivity are obtained yet at the price of a lower effective bitrate. The Rx sensitivity when reducing BW<sub>ONU</sub> from 50% to 25% improves by 6dB for BPSK. Similar values are obtained for DS (Fig. 5). For QPSK, the Rx sensitivity is as low as -24.5dBm with BW<sub>ONU</sub>=25%, almost 8dB better than with BW<sub>ONU</sub>=50%. The performance is slightly better for ONU<sub>1</sub> which operated in baseband than for ONU<sub>2</sub> because of small drifts in  $f_{IF2}$  and the non-ideal laser response which caused some distortion in the higher part of the spectrum.

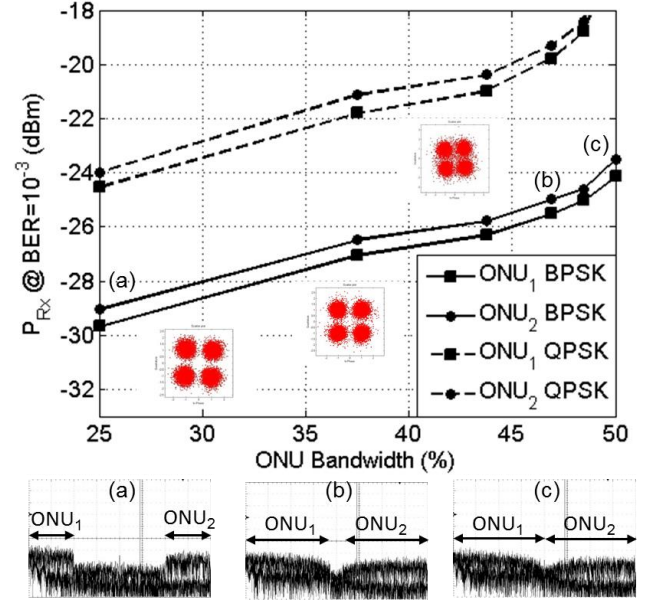


Fig. 10. Rx sensitivity at BER=10<sup>-3</sup> against BW<sub>ONU</sub> for both ONUs with BPSK and QPSK modulation in multiband OFDM. The insets show the spectrum of each ONU contribution in the Rx signal.

We also tested the UL with ONUs processing the complete signal with BPSK, QPSK, and several ZP percentages. The Rx sensitivity against BW<sub>ONU</sub> measured at the OLT for each ONU is plotted in Fig. 11. The results were around 1dB better than the multiband OFDM due to the frequency drifts in the RF mixer. For BW<sub>ONU</sub> > 45% the non-ideal electrical filters used in multiband OFDM to confine and limit the BW of each ONU did not remove the spectral tails completely producing overlapping when the UL contributions were combined. Thus, in these cases the Rx sensitivity of the ONUs processing the whole OFDM signal, improved by 2dB. However, the multiband OFDM has the relevant advantage of lowering the ONU complexity by reducing the FFT size through the help of an RF mixer. This translates directly into the power consumption which is also lowered.

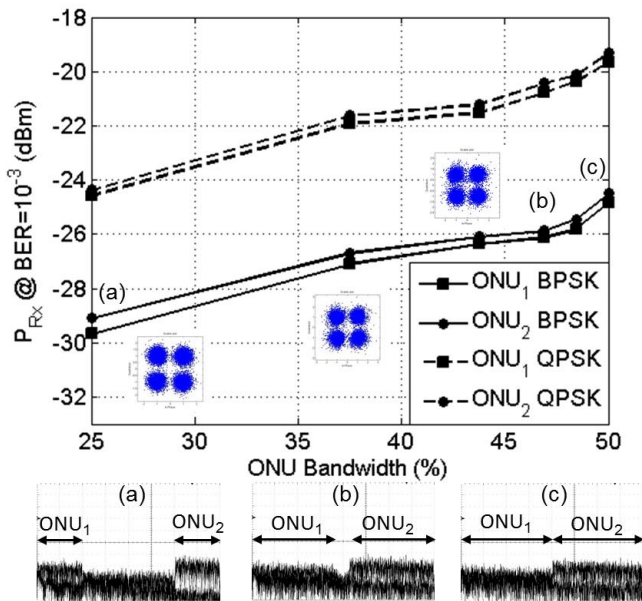


Fig. 11. Rx sensitivity at  $\text{BER}=10^{-3}$  against effective data BW for both ONUs with BPSK and QPSK modulation with each ONU processing the whole BW. The insets show the spectrum of each ONU contribution in the detected signal.

To further evaluate the relation between the Rx sensitivity, modulation format and active SC, the experiment was extended to 8-PSK and 16-QAM. Fig. 12 summarizes the Rx sensitivity needed at  $\text{BER}=10^{-3}$  (level lines) as a function of both the modulation format and  $\text{BW}_{\text{ONU}}$  considering an average over the two ONUs.

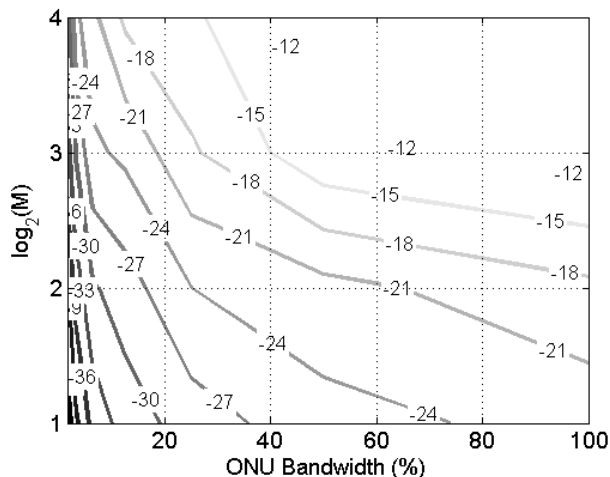


Fig. 12. Rx sensitivity at  $\text{BER}=10^{-3}$  level lines (in dBm) as a function of modulation format and  $\text{BW}_{\text{ONU}}$ . (M: modulation bits).

The lines in Fig. 12 can be used to allocate the active SC and modulation format for each ONU according to the users BW need and available power budget. The negotiation can be carried out at the registration process or dynamically during operation. As an example, for the ODN shown in Fig. 2, if  $\text{ONU}_1$  transmits and receives a QPSK signal with  $\text{BW}_{\text{ONU}}=3.12\%$  ( $P_{\text{Rx}}=-33\text{dBm}$ ) and  $\text{ONU}_2$  uses BPSK with  $\text{BW}_{\text{ONU}}=96.8\%$  ( $P_{\text{Rx}}=-23\text{dBm}$ ), there is a difference of 10dB in the Rx power needed. This value translates into a fiber length separation of 50km or an extra splitting ratio of 1:8.

Therefore, the differential link-loss can be compensated and both users are detected properly.

As a final test, the SC allocation was assessed experimentally in UL by transmitting a short video signal. The complete description and results can be seen in [26].

## V. CONCLUSION

A statistical OFDMA PON with multiband ONUs based on simple independent non-preselected DFB lasers was experimentally evaluated. The assessment included both DS and UL in separate optical bands with almost symmetrical Rx sensitivities of  $-25\text{dBm}$  at  $\text{BER}=10^{-3}$  with BPSK. A penalty of 5dB was obtained when the modulation format was extended to QPSK. The total effective capacity was 2.5/5 Gb/s for BPSK and QPSK respectively. The digital SC allocation was also tested and the Rx sensitivity improved up to 2dB when compared with the multiband technique. However, the advantage of the latter was that it allowed the ONU to process only its intended BW. The technique placed the ONU BW in its corresponding spectral band with the aid of an RF mixer, thus reducing the complexity and energy consumption. For the UL, a spectral BG of 6.25% was required to detect simultaneously both ONUs at the OLT with QPSK while keeping the penalty below 5dB with respect to BPSK. The flexibility of OFDM to grant different SC and modulation formats independently to ONUs was also studied. The Rx sensitivity was enhanced by almost 6dB when  $\text{BW}_{\text{ONU}}$  was reduced from 50% to 25%. The results showed that the statistical OFDM PON could adapt to the users BW requirement and power budget availability. As a result, the BW can be allocated intelligently and dynamically through media access control protocols to compensate a differential link-loss of up to 18dB among the users in the PON.

## ACKNOWLEDGMENT

This work was supported in part by the European FP-7 projects ACCORDANCE and COCONUT, the Spanish Ministry of Science and Innovation under Grant TEC2011-25215 (ROMULA) and Mexican Science and Technology Council (CONACYT) under grant 185291.

## REFERENCES

- [1] D. Qian, N. Cvijetic, J. Hu, and T. Wang, "A novel OFDMA-PON architecture with source-free ONUs for next-generation optical access networks," *IEEE Photon. Technol. Lett.*, vol.21, pp. 1265-1267, Sept. 2009.
- [2] N. Cvijetic, "OFDM for next-generation optical access networks," *IEEE J. Lightwave Technol.*, vol. 30, pp.384-398, Feb. 2012.
- [3] K. Kanonakis, I. Tomkos, H. G. Krimmel, F. Schaich, C. Lange, E. Weis, J. Leuthold, M. Winter, S. Romero, P. Kourtessis, M. Milosavljevic, I. N. Cano, and J. Prat, "An OFDMA-based optical access network architecture exhibiting ultra-high capacity and wireline-wireless convergence," *IEEE Commun. Mag.*, vol. 50, pp. 71-78, Aug. 2012.
- [4] W. Lim, P. Kourtesis, M. Milosavljevic, and J. M. Senior, "Dynamic subcarrier allocation for 100Gbps, 40 km OFDMA-PONs with SLA and CoS," *IEEE J. Lightwave Technol.*, vol. 31, pp. 1055-1062, April 2013.
- [5] J. von Hoyningen-Huene, H. Griesser, M. H. Eiselt, W. Rosenkranz, "Experimental demonstration of OFDMA-PON

- uplink-transmission with four individual ONUs,” presented at OFC 2013, Anaheim CA, Mar. 19-21, paper OTh3A.2.
- [6] C. Ruprecht, Y. Chen, D. Fritzsche, J. von Hoyningen-Huene, N. Hanik, E. Weis, D. Breuer, W. Rosenkranz, “37.5-km urban field trial of OFDMA-PON using colorless ONUs with dynamic bandwidth allocation and TCM,” presented at OFC 2014, San Francisco, CA, Mar. 11-13, paper Th3G.5.
- [7] I. Cano, M. C. Santos, V. Polo, and J. Prat, “Dimensioning of OFDMA PON with non-preselected independent ONUs sources and wavelength-control,” *Optics Express*, vol. 20, pp. 607-613, Jan. 2012.
- [8] W. Poehlmann and T. Pfeiffer, “Demonstration of wavelength-set division multiplexing for a cost effective PON with up to 80Gbit/s upstream bandwidth,” presented at ECOC 2011, Geneva, Switzerland, Sept. 18-22, paper We.9.C.1.
- [9] N. Cheng, G. Wei, and F. Effenberger, “Dynamic spectrum managed passive optical networks,” *IEEE Commn. Mag.*, vol. 49, pp. 86-93, Nov. 2011.
- [10] P. Vetter, “Next generation optical access technologies,” presented at ECOC 2012, Amsterdam, Netherlands, Sept. 16-20, paper Tu.3.G.1.
- [11] B. Charbonnier, A. Lebreton, P. Chanclou, G. Beninca, S. Mexezo, R. Dong, and J. LeMasson, “Low complexity FDM/FDMA approach for future PON,” presented at OFC 2013, Anaheim, CA, Mar. 19-21, paper OTh3A.7.
- [12] I. Cano, X. Escayola, P. Schindler, M. Santos, V. Polo, J. Leuthold, and J. Prat, “Experimental demonstration of multi-band upstream in statistical OFDM-PONs and comparison with digital subcarrier assignment,” presented at OFC 2014, San Francisco, CA, Mar. 11-13, paper Th3G.4.
- [13] P. Chanclou, A. Cui, F. Geilhardt, H. Nakamura, and D. Nettet, “Network operator requirements for the next generation of optical access networks,” *IEEE Network*, vol. 26, pp. 8-14, Mar. 2012.
- [14] I.N. Cano, A. Peralta, V. Polo, X. Escayola, M. Santos, J. Prat, “Differential link-loss compensation through dynamic bandwidth assignment in statistical OFDMA-PON,” presented at OFC 2013, Anaheim CA, Mar. 19-21, paper OTh3A.5
- [15] A. Dochhan, H. Griesser, L. Nadal, M. H. Eiselt, M. Svaluto, J. P. Elbers, “Experimental investigation of discrete multitone transmission in the presence of optical noise and chromatic dispersion,” presented at OFC 2014, San Francisco, CA, Mar. 11-13, paper Tu2G.7.
- [16] S. L. Jansen, B. Spinnler, I. Morita, S. Randel, and H. Tanaka, “100GbE: QPSK versus OFDM,” *Optical Fiber Technology*, vol. 15, pp. 407-413, Dec. 2009.
- [17] J. Tang, E. Hugues-Salas, R. P. Giddings, “First experimental demonstration of real-time adaptive transmission of 20Gb/s dual-band optical OFDM signals over 500m OM2 MMFs,” presented at OFC 2013, Anaheim, CA, Mar. 19-21, paper OTh3A.1.
- [18] V. Polo, P. Borotau, A. Lerín, and J. Prat, “DFB laser reallocation by thermal wavelength control for statistical udWDM in PONs,” accepted for presentation at ECOC 2014.
- [19] D. van Veen, W. Pöhlmann, J. Galaro, B. Deppisch, A. Duque, M. F. Lau, B. Farah, T. Pfeiffer, and P. Vetter, “System demonstration of a time and wavelength-set division multiplexing PON,” presented in ECOC 2013, London, UK, Sept. 22-26, paper We.3.F.2.
- [20] S. Kaneko, T. Yoshida, S. Furusawa, M. Sarashina, H. Tamai, A. Suzuki, T. Mukojima, S. Kimura, N. Yoshimoto, “First  $\lambda$ -tunable dynamic load-balancing operation enhanced by 3-sec bidirectional hitless tuning on symmetric 40-Gbit/s WDM/TDM-PON,” presented in OFC 2014, San Francisco, CA, Mar. 9-13, paper Th5A.4.
- [21] “Virtex-6 family overview,” Xilinx Inc. Jan. 2010.
- [22] C. Desem, “Optical interference in subcarrier multiplexed systems with multiple optical carriers,” *IEEE J. Select. Areas Commun.*, vol. 8, pp. 1290-1295, Sept. 1990.
- [23] X. Q. Jin and J. M. Tang, “Experimental investigations of Wavelength Spacing and Colorlessness of RSOA-Based ONUs in Real-Time Optical OFDMA PONs”, *IEEE J. Lightwave Technol.*, vol. 30, pp. 2603-2609, Aug. 2012.
- [24] X. Q. Jin, J. Groenewald, E. Hughes-Salas, R. P. Giddings, and J. M. Tang, “Upstream power budgets of IMDD optical OFDMA PONs incorporating RSOA intensity modulator-based colorless ONUs,” *IEEE J. Lightwave Technol.*, vol. 31, pp. 1914-1920, June 2013.
- [25] B. J. C. Schmidt, A. J. Lowery, and J. Armstrong, “Experimental demonstrations of electronic dispersion compensation for long-haul transmission using direct-detection optical OFDM,” *IEEE J. Lightwave Technol.*, vol. 26, pp. 196-203, Jan. 2008.
- [26] I. Cano, X. Escayola, P. Schindler, M. Santos, V. Polo, J. Leuthold, and J. Prat (2013, Dec. 6). Upstream statistical OFDM low-cost solution [Online]. Available: <https://www.youtube.com/watch?v=0lbuYu1Ccxk>